

ANNALS OF THE NEW YORK ACADEMY OF SCIENCES

Issue: *Analysis of Cardiac Development*

Multiscale modeling of metabolism, flows, and exchanges in heterogeneous organs

James B. Bassingthwaighe, Gary M. Raymond, Erik Butterworth, Adam Alessio, and James H. Caldwell

Departments of Bioengineering, Medicine, and Radiology, University of Washington, Seattle, Washington, USA

Address for correspondence: Prof. James B. Bassingthwaighe, M.D., Ph.D., Department of Bioengineering, University of Washington, Box 35-5061, Seattle, WA 98195-5601. jbb2@u.washington.edu

Large-scale models accounting for the processes supporting metabolism and function in an organ or tissue with a marked heterogeneity of flows and metabolic rates are computationally complex and tedious to compute. Their use in the analysis of data from positron emission tomography (PET) and magnetic resonance imaging (MRI) requires model reduction since the data are composed of concentration–time curves from hundreds of regions of interest (ROI) within the organ. Within each ROI, one must account for blood flow, intracapillary gradients in concentrations, transmembrane transport, and intracellular reactions. Using modular design, we configured a whole organ model, GENTEX, to allow adaptive usage for multiple reacting molecular species while omitting computation of unused components. The temporal and spatial resolution and the number of species are adaptable and the numerical accuracy and computational speed is adjustable during optimization runs, which increases accuracy and spatial resolution as convergence approaches. An application to the interpretation of PET image sequences after intravenous injection of $^{13}\text{NH}_3$ provides functional image maps of regional myocardial blood flows.

Keywords: multiscale modeling; cardiovascular system; myocardial blood flows; computational biology; capillary–tissue exchange; JSim simulation analysis; optimization; positron emission tomography; magnetic resonance imaging

Introduction

The physiome project and the modeling of *in vivo* data

Multiscale modeling is essential to achieving the goals of the Physiome Project. The “physiome” is the quantitative mathematical description of the functional behavior of the physiologic state of an individual of a species. It would ideally describe the real-time physiology of an intact organism; the information contained should be self-consistent with the structure (genome, proteome, and morphome) and the laws of physics and chemistry. The term comes from *physio-* (life) and *-ome* (as a whole). In its broadest sense, the physiome should define relationships from genome to organism and from functional behavior to gene regulation. In the context of the Physiome Project, it includes integrated models of components of organisms, such as particular organs or cell systems, and biochemical or endocrine systems.

The Physiome Project, or better-phrased, *Projects*, is a loosely knit worldwide effort to develop models and model databases with experimental data. Our efforts on the Cardiome Project⁵ are only one of several. The models are to facilitate understanding of the functions of cells and organs and organisms, and to aid in the design of experiments to fill in gaps in knowledge and understanding. The project is focused on developing and archiving physiologic models, and providing repositories of databases, linking experimental information and computational models from many laboratories into self-consistent frameworks. Through accurate, complete modeling and disseminating reproducible models as the current quantitative working hypotheses for particular systems, and through the provision of reliable, curated data, and models in public databases, biological scientists will be better able to integrate information, analyze data, and improve predictive capability.

Model databases greatly facilitate the advancement of the science. Models for cardiovascular and neurologic systems are prominent in the history of physiology. Fields in which good instrumentation has provided quantitative measures obviously have the benefit of an abundance of solid data on which to base hypotheses. In particular, electrophysiology has seen great advances, and biophysically based models are available for a host of situations. The PhysioNet database (www.physionet.org), originally created to disseminate electrophysiologic data, such as electrocardiograms, has evolved so that now it contains models and modeling systems as well. QKDB, the quantitative kidney database (www.physiome.ibisc.fr/qkdb/) is a repository of data and models in which the model serves as the entry to a library of information and literature on the data and parameters of the models.

The Physiome site at University of Washington (www.physiome.org) provides a long list of models and databases. It provides more than 450 models that can be run over the web as Java applets, modified (parameters or all parts of the code), and then downloaded to the visitor's computer, and run via the freely available Java-based simulation system JSim. All of the models archived at this site are provided with units, which JSim checks for computational errors with unit balance checking and automatic unit conversion.

The CellML website (the IUPS site www.physiome.org.nz) contains about 800 models, mostly at the level of cellular reactions. They can be downloaded and translated into computable code. About half are curated, and most of these now run on other platforms. These are all either ODEs (ordinary differential equations) or algebraic equations and require only a good ODE solver. The same applies to the models on the more extensive SBML (Systems Biology Markup Language) site at sbml.org/index.psp. Only a fraction of these models is curated; they are being provided with units. A selection of them (now more than 80 models) has been carefully curated and is available at www.ebi.ac.uk/biomodels/, the BioModels database.

Electrophysiological modeling is having a profound impact on research studies, on clinical applications, and on the pharmaceutical industry's choices of drugs to target arrhythmias. The introduction to the cardiovascular models at the IUPS site

suggests that this should happen even more broadly, and state that:

"An integration of large-scale computer modeling with experimental studies is necessary to understand the mechanisms that underlie re-entrant arrhythmia and fibrillation in the heart. . . .

There are three linked goals:

1. To understand how cardiac arrhythmias at the whole heart level can occur as a result of ion channel mutations, ischemia, and drug toxicity.
2. To demonstrate the use of integrative multi-scale modeling (at the levels of proteins, biochemical pathways, cells, tissues, and whole organs) as 'proof of concept' for more detailed physiome projects.
3. To provide electrocardiologists with web-accessible software tools and databases for use in generating new hypotheses and interpreting complex experimental data."

These statements indicate that multiscale modeling is a principal tool in such efforts, and that most comprehensive and utilitarian models will have to cover the levels from proteins and substrates to the whole organ, or to a multiorgan system, such as the endocrine system. The quote above defined the effort as international collaboration between Auckland and Oxford, an example typical of most multiscale projects these days.

The physiome modeling spans genome to function, including responses to the environment

In principle the ideas and models of the Physiome Project should span physiology from early embryonic development to senescence and death. Environmental factors are paramount over the lifespan, having major influences on rates of expression and the physiologic state (awareness, physical fitness, level of stress) and the responses to disease and injury. The key power of integrative modeling is that it can ultimately provide an understanding of the *in vivo* state. This is where science is going; one knows well enough that isolated molecules (enzymes, channels, receptors) behave differently in the test tube than they do in their normal settings inside cells or as integral proteins in membranes. Likewise, behavior of the individual cell in culture is vastly different from

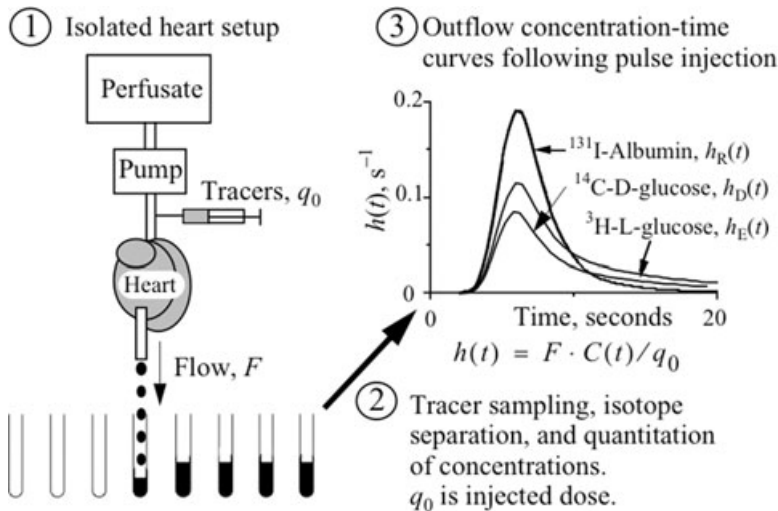


Figure 1. The multiple indicator dilution experiment. (1) A set of tracers demarcating different aspects of the system are injected simultaneously into the inflowing arterial blood and the outflow is sampled continuously. (2) Outflow concentrations are obtained at each time point for each tracer and its metabolites. (3) The concentration time curves are normalized to the fraction of injected dose appearing in the outflow per unit time, and the system responses.

that of the same cell in the structured assemblage of a tissue composed of multiple cell types, each signaling to the others. Even as simple an organ as the heart behaves substantially differently when blood-perfused outside of the body, than when it is reacting to a variety of neurohormonal and direct mechanical influences, such as venous pressure filling the ventricles during diastole and of aortic blood pressure resisting aortic valve opening and ejection of blood from the left ventricular (LV) cavity. Thus the goal of the biological experimenter is either to acquire the data *in vivo* or to translate from the observed *in vitro* or *in cultura* state to the *in vivo* state, which is often difficult.

An example is discussed in the following section: a generic organ-level model system, GENTEX, for cardiac regional flows, exchanges, and metabolism.

Multiscale models

The input/output relationship in organs *in vivo* and *in vitro*: the multiple indicator dilution study

The multiple indicator dilution (MID) experiment is based on traditional engineering approaches to probing a linear system: determine the relationship between a known input and an observed output to determine the system characteristics. The MID experiment (Fig. 1) is based on linear systems analysis,

just like Fourier or other transform techniques. An input $f(t)$ convoluted with the system impulse response $h(t)$ predicts the output function $g(t)$; or, alternatively written, $g(t) = f(t) * h(t)$, where the asterisk denotes the convolution integration.

The theoretical bases for the analysis are provided by Bassingthwaighe and Goresky.^{1,4} Multiple metabolites, in addition to the injected tracers, may also be produced and are invaluable data since they define the transport and reaction delays for the product. In such studies there are ordinarily at least two reference indicators: an intravascular one to define the transport function (delay, dispersion) due to carriage in the blood, ^{131}I -albumin (MW = 68,000) in the figure, and an extracellular tracer, ^3H -L-glucose in Figure 1, chosen because it has the same molecular weight (182 daltons) and diffusive characteristics as the substrate of prime interest, D-glucose (labeled with ^{14}C -carbon). The L-glucose transport function describes the processes of permeation across the capillary wall through the interendothelial clefts and distribution throughout the interstitial space, the ISF. Because the molecular weights of the tracer-labeled D- and L-glucose are identical, the L-glucose has the same time course in plasma and ISF as does the D-glucose, thus providing an ideal reference for assessing the rate of uptake of the D-glucose into the endothelial cells (ECs or subscripted ec) and cardiomyocytes.

GENTEX, a generic organ-level model system
Our model^{2,6} for data analysis, GENTEX, is a multiscale, multicomponent construct; it includes a combination of convection, permeation, diffusion, transmembrane transport, and intracellular reactions—up to twelve molecular species. It models:

1. Vascular transport in arteries and veins, with subsets of arterioles and venules having differing flows to account for heterogeneity in regional myocardial blood flows.¹⁰ This is done by having up to twenty independent capillary–tissue exchange units, each differing from the others only with respect to the local flow, important for a wide range of small hydrophilic solutes.^{9,12} The experimentally observed probability density functions of regional flows are represented by a weighting function approximating the distribution around the known mean flow, using only enough paths, often as few as 5 or 7, to capture the form of the distribution.
2. Axially distributed blood–tissue exchange units accounting for intravascular and extravascular concentration gradients (Fig. 2), and allowing axial diffusion in all regions. A LaGrangian sliding fluid algorithm gives rapid computation.³
3. Units composed of five regions radially: red blood cells (RBCs), plasma (p), endothelial cells (ec or ECs), interstitial fluid space (ISF), and the parenchymal cells (pc or PCs), the cardiomyocytes.
4. Transmembrane transport by facilitated, competitive, or passive transport.
5. Reactions that are first-order or enzymatically facilitated. These may be individual for each solute or in sequences or in branched paths with intracellular sequestration as for adenosine entering into the ATP pool.
6. Adsorption to ligand-specific intracellular binding sites for each reactant.

GENTEX handles up to five metabolizing substrates, either as individual species or up to five reacting species in series. The model includes the reference intravascular and an extracellular species. Cr-labeled hemoglobin can serve as a RBC reference tracer, which is important when solutes of interest enter the RBCs; RBC velocities in capillaries and

small vessels are higher than that of plasma. Each of the five reacting species is modeled for nontracer as well as tracer species, allowing specification of the radioactivity of each one, and accounting for competition between tracer and other substance. Thus, the total number of species handled as the central time- and space-dependent variables is twelve. Parameters, including flow, are considered as constants, some of which are measured, whereas others are estimated from the data.

The blood tissue exchange (BTEX) unit model for each solute species is an extension of the 1989 model² for capillary plasma, endothelium, ISF, and myocytes, adding the erythrocytes and accounting for RBC and plasma velocities separately to describe hematocrit reduction in microvessels. The input to each BTEX unit is by convection into the upstream end of the capillary. Model assumptions are: steady flow, rapid relaxation of radial concentration gradients in each physical region (perpendicular to the direction of flow), spatially uniform coefficients for permeation, diffusion, and consumption. BTEX units account for conductances, PS , across the barriers between the regions, the regional volumes of distribution (V'), the dispersion in the axial direction (D), and consumption (G). Each PS and G can be modified at runtime to choose a more complex algorithm for carrier-mediated transport or enzymatically facilitated reaction. The GENTEX model accounts for chemical reactions, for mass balance and concentration-dependencies in reactions, binding, and transporter-mediated permeation. The tracer submodel uses linear coefficients slaved to the parent chemical model for each reactant species.

Parameters used in fitting data are:

F_p	flow of solute-containing plasma or perfusate, $\text{mL g}^{-1} \text{min}^{-1}$
PS_{RBC}	permeability surface area product for erythrocytes, $\text{mL g}^{-1} \text{min}^{-1}$
PS_g	permeability surface area product for passive transport between the plasma and ISF regions through the gaps or clefts between adjacent endothelial cells, $\text{mL g}^{-1} \text{min}^{-1}$

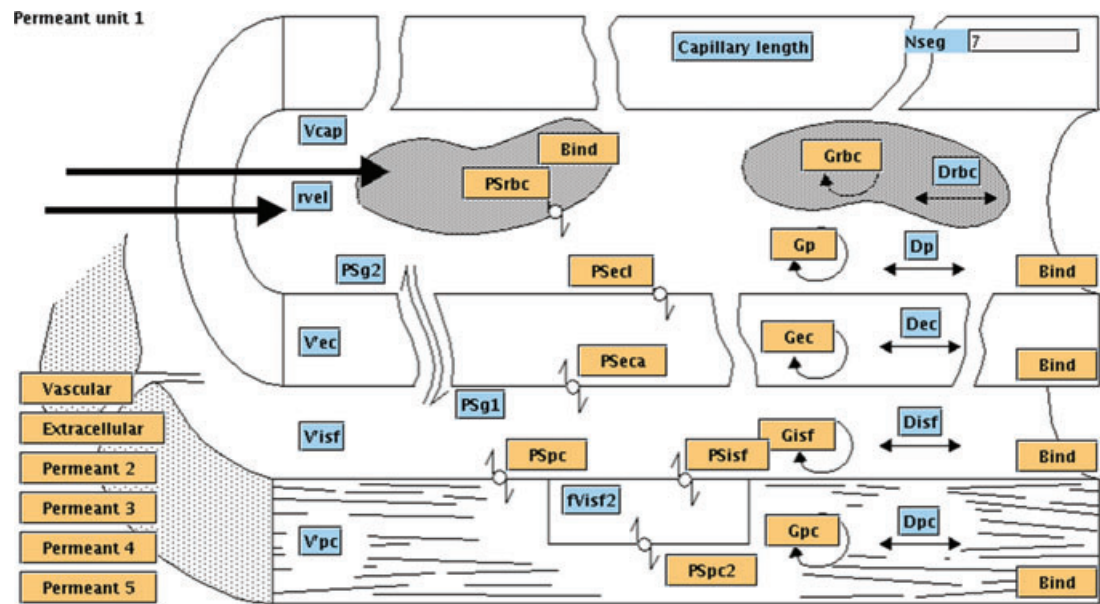


Figure 2. Parameter entry interface for one substrate’s capillary blood–tissue exchange (BTEX) unit of the generic multiscale multicapillary model, GENTEX. Each unit accounts for 12 species: (intravascular and extracellular reference tracers) and 5 dual (tracer and non-tracer chemical) reacting species that enter cells (RBCs and endothelial and parenchymal cells). This is the generic five-region, four-barrier model for blood–tissue exchange. The analysis used a set of such modules in parallel to account for the normal myocardial flow heterogeneity. (From Bassingthwaighte *et al.*⁶ Reproduced by permission.)

PS_{ecl}	permeability surface area product for endothelial cell luminal surface, $\text{mL g}^{-1} \text{min}^{-1}$	interstitial space (isf), and parenchymal cells (pc). A virtual volume will exceed the actual volume if its equilibrium total concentration of bound plus free solute is higher than in the plasma, which is the reference space. Numerically, $V'_{reg} = \lambda$ times V_{reg} , where λ is a partition coefficient, $\lambda = C_{reg}/C_p$ at equilibrium.
PS_{eca}	abluminal endothelial permeability surface area product, $\text{mL g}^{-1} \text{min}^{-1}$ (assumed = PS_{ecl})	
PS_{pc}	permeability surface area product for parenchymal cells (myocytes), $\text{mL g}^{-1} \text{min}^{-1}$	
G_{reg}	regional consumptions, or gulosesities, $\text{mL g}^{-1} \text{min}^{-1}$. The reaction may be Michaelis–Menten or first order. The subscript reg for region refers to RBC, p, ec, isf, or pc.	
D_{reg}	diffusion coefficient, $\text{cm}^2 \text{s}^{-1}$ for a region	
V_p	intracapillary plasma volume (mL g^{-1})	
$V'_{RBC}, V'_{ec}, V'_{isf}, V'_{pc}$	virtual volumes of distribution, mL g^{-1} of erythrocytes (RBC), endothelial cells (ec),	

The regional concentrations, $C_{reg}(x, t)$ moles per milliliter, are a function of capillary axial position, x , and of time, t . The partial differential equation (PDE) for the concentration of a solute is: in the capillary plasma (p),

$$\frac{\partial C_p}{\partial t} = -\frac{F_p L}{V_p} \cdot \frac{\partial C_p}{\partial x} - \frac{P S_g}{V_p} (C_p - C_{isf}) - \frac{P S_{ecl}}{V_p} (C_p - C_{ec}) - \frac{G_p}{V_p} C_p + D_p \frac{\partial^2 C_p}{\partial x^2}$$

in the erythrocytes (RBC),

$$\frac{\partial C_{\text{RBC}}}{\partial t} = -\frac{F_{\text{RBC}} L}{V_{\text{RBC}}} \cdot \frac{\partial C_{\text{RBC}}}{\partial x} - \frac{P S_{\text{RBC}}}{V'_{\text{RBC}}} (C_{\text{RBC}} - C_p) - \frac{G_{\text{RBC}}}{V'_{\text{RBC}}} C_{\text{RBC}} + D_{\text{RBC}} \frac{\partial^2 C_{\text{RBC}}}{\partial x^2}$$

in the endothelial cells (ec),

$$\frac{\partial C_{\text{ec}}}{\partial t} = -\frac{P S_{\text{ecI}}}{V'_{\text{ec}}} (C_{\text{ec}} - C_p) - \frac{P S_{\text{eca}}}{V'_{\text{ec}}} (C_{\text{ec}} - C_{\text{isf}}) - \frac{G_{\text{ec}}}{V'_{\text{ec}}} C_{\text{ec}} + D_{\text{ec}} \frac{\partial^2 C_{\text{ec}}}{\partial x^2}$$

in the interstitial fluid (isf),

$$\frac{\partial C_{\text{isf}}}{\partial t} = -\frac{P S_g}{V'_{\text{isf}}} (C_{\text{isf}} - C_p) - \frac{P S_{\text{eca}}}{V'_{\text{isf}}} (C_{\text{isf}} - C_{\text{ec}}) - \frac{P S_{\text{pc}}}{V'_{\text{isf}}} (C_{\text{isf}} - C_{\text{pc}}) - \frac{G_{\text{isf}}}{V'_{\text{isf}}} C_{\text{isf}} + D_{\text{isf}} \frac{\partial^2 C_{\text{isf}}}{\partial x^2}$$

and in the parenchymal cells (pc),

$$\frac{\partial C_{\text{pc}}}{\partial t} = -\frac{P S_{\text{pc}}}{V'_{\text{pc}}} (C_{\text{pc}} - C_{\text{isf}}) - \frac{G_{\text{pc}}}{V'_{\text{pc}}} C_{\text{pc}} + D_{\text{pc}} \frac{\partial^2 C_{\text{pc}}}{\partial x^2}$$

L is a capillary length, in the heart averaging 0.8 mm, and a position x/L is a fraction of the capillary length. The erythrocyte velocity, $F_{\text{RBC}} L/V_{\text{RBC}}$, is faster than plasma velocity and the intracapillary hematocrit, $\text{Hct}_{\text{cap}} = V_{\text{RBC}}/(V_p + V_{\text{RBC}})$ is less than the large vessel hematocrit, Hct_{LV} . This speedier RBC velocity, measurable in vessels less than 200 microns in diameter, persists even into capillaries where there is an RBC-free layer of plasma within the endothelial glycocalyx lining the capillaries.¹⁴ The direct path through the gaps between the endothelial cells allowing direct plasma–isf exchange, PS_g , bypassing the ECs, makes this model different than one with a set of concentric volumes, and permits accounting for molecular size.⁷

The heterogeneity model

Accounting for heterogeneity in a fully knowledgeable way is probably impossible: the result is that arbitrary choices have to be made. Heterogeneity of

regional flows is known from experimental data in the hearts of live awake exercising baboons;¹⁰ the coefficient of variation (standard deviation divided by the mean) is about 25%. The relative regional flows are spatially stable, the temporal variation being only 10 to 15%. This is accounted for by using a multipath model with a weighting of the distribution of independent flows matching the observed distribution of flows. Since it is desirable to minimize the number of parallel paths, one must choose how precisely to match the distribution; an even spacing in mean transit times works well.¹¹

The deeper question is: what is the distribution of metabolic rates? Fortunately for parsimony in the modeling, both fatty acid uptake⁸ and oxygen metabolism¹³ are both approximately linearly related to the flow,⁵ thus this same relationship is assumed for all metabolic processes. Our general assumption is certainly not proven, but the alternative assumption that all regions have similar metabolic rates is denied by data on regional flow versus regional uptake of glucose or deoxyglucose or fatty acid or regional oxygen consumption.

Optimization under constraints: reducing the degrees of freedom

A glance at the capillary–tissue model figure and the list of parameters would lead one to throw up one's hands at the prospect of fitting data meaningfully when there are so many parameters. Fortunately, the number of free parameters is *much fewer* than the number of molecular species times the number on the list. Further, data constrain many parameters; data to be used include not only the multiple indicator dilution data, but also the known anatomic data, the binding affinities of enzymes and transporters, the locations for reactions, the conservation of reactants and products, intratissue diffusion coefficients, and often the concentrations of binding sites, as for hemoglobin, albumin, and myoglobin, each in its known location (RBCs, plasma, and cardiomyocyte cytosol).

The anatomic measures should be considered as data.¹⁵ Total water content of a given tissue is almost constant: in the the dog heart it is 0.77 ± 0.01 mL per gram of tissue; the density is 1.055 ± 0.005 g/mL. Using these observations, tracer and stereologic assessments of volumes, and the known densities of water, fat, protein, and salts, one can optimize the matrix of information to provide the

best estimates of the myocardial distributions of density, volume, and composition (water, protein, fat, salts) in each tissue component (RBC, plasma, ISF, cells, and the cell components, cytoplasm, mitochondria, and sarcoplasmic reticulum). These values are then used to parameterize the biochemical models, and in translating from gross tissue ATP concentrations to cytosolic concentrations.

Other constraining influences are thermodynamic and physical. For example, the ratio of permeabilities of any pair of solutes traversing the interendothelial cellular clefts is the ratio of their free diffusion coefficients in water, with minor adjustments for steric hindrance made by a hydrodynamic correction.⁷ Thermodynamic constraints are applied to all biochemical reactions to adhere to known equilibrium dissociation constants and the reversibility of reactions (Haldane constraints).

A major constraint is obtained by fitting simultaneously multiple sets of indicator dilution data on a set of reactants, so that all lend their influence on the common set of parameters, as has been found valuable for parameterizing the purine nucleoside network in endothelial cells and myocytes.⁶ When one has two reference tracers, an injected tracer substrate, and three tracer metabolic products, for a total of 6 time–activity curves of about 60 points each, then one has 360 data points from which to obtain estimates of around a dozen partially constrained parameters. Under such circumstances the confidence ranges on the estimates are comfortably narrow.

Adaptive reconfiguration of the model can be used during optimization runs. The computation time goes up as the square of the number of axial grid elements, so at the beginning of the optimization run one can gain speed by using only 5 to 10 axial elements and one pathway. Then as the model fit to the data converges, one increases the number of pathways to 3 and then to 5, and the number of grid elements to solve the PDEs to 15 or 20, thereby increasing the accuracy of the model representation of the physiology.

Applications of the multiscale GENTEX model

Use of the GENTEX model is not limited to MID-type data, although that is the type of data that puts the greatest demand on the fidelity of the model. In fact, it was the shapes of the indicator dilution curves that forced us to use the multicapillary models ac-

counting for flow and metabolic heterogeneity. The clinical applications are in positron emission tomographic (PET) imaging and in magnetic resonance imaging (MRI). Modeling analysis is common for PET, but only relatively recently has the nuclear medicine community become aware that it should use models accounting for gradients in concentrations within the blood–tissue exchange unit rather than using a lumped, stirred-tank model. Lumped models implicitly assume that the concentration near the input is identical to that at the output (having no internal gradient and assuming a discontinuity in concentration at the entrance); the result is that the parameters estimated from them are incorrect, strikingly so for permeabilities, though only moderately erroneous for consumption rates. PET is excellent for noninvasive metabolic measures, but only physiologically realistic models give good parameter estimates.

MRI can also be used for obtaining quantitative data on transient concentrations of contrast agents, such as for the estimation of tissue blood flow, where GENTEX has been used.¹⁶ The GENTEX model allows for the exchange of spin-labeled water across the cell membranes, while the usual contrast agents such as Gd-labeled DPTA are limited to the extracellular space. The modeling with GENTEX, therefore, provides improved accuracy in flow estimates, overcoming a systematic error of 10 to 20% using compartmental models without this consideration.

This general purpose model is applicable to clinical data analysis, for example, as a part of a semi-automated system for analyzing a sequence of PET images after intravenous injection of $^{13}\text{NH}_3$. The product is functional image maps of regional myocardial blood flows (rMBFs). For this purpose we have developed a semi-automated approach to allow rapid evaluations and reporting of quantitative measures of rMBFs in visual and numerical form: the Quantitative Perfusion Program (QPP) operates on a four-dimensional PET or MR image set after bolus injection of radiotracer, initially presenting the user with a best positioning of the heart displayed as three orthogonal projections derived from the transaxial image set (Fig. 3, left). The user can refine the position and proceed to create a set of images relative to the cardiac short axis, vertical and horizontal long axes, and time course of radiotracer transit through the chambers and myocardium. The user then positions a 3D region of interest (ROI) in

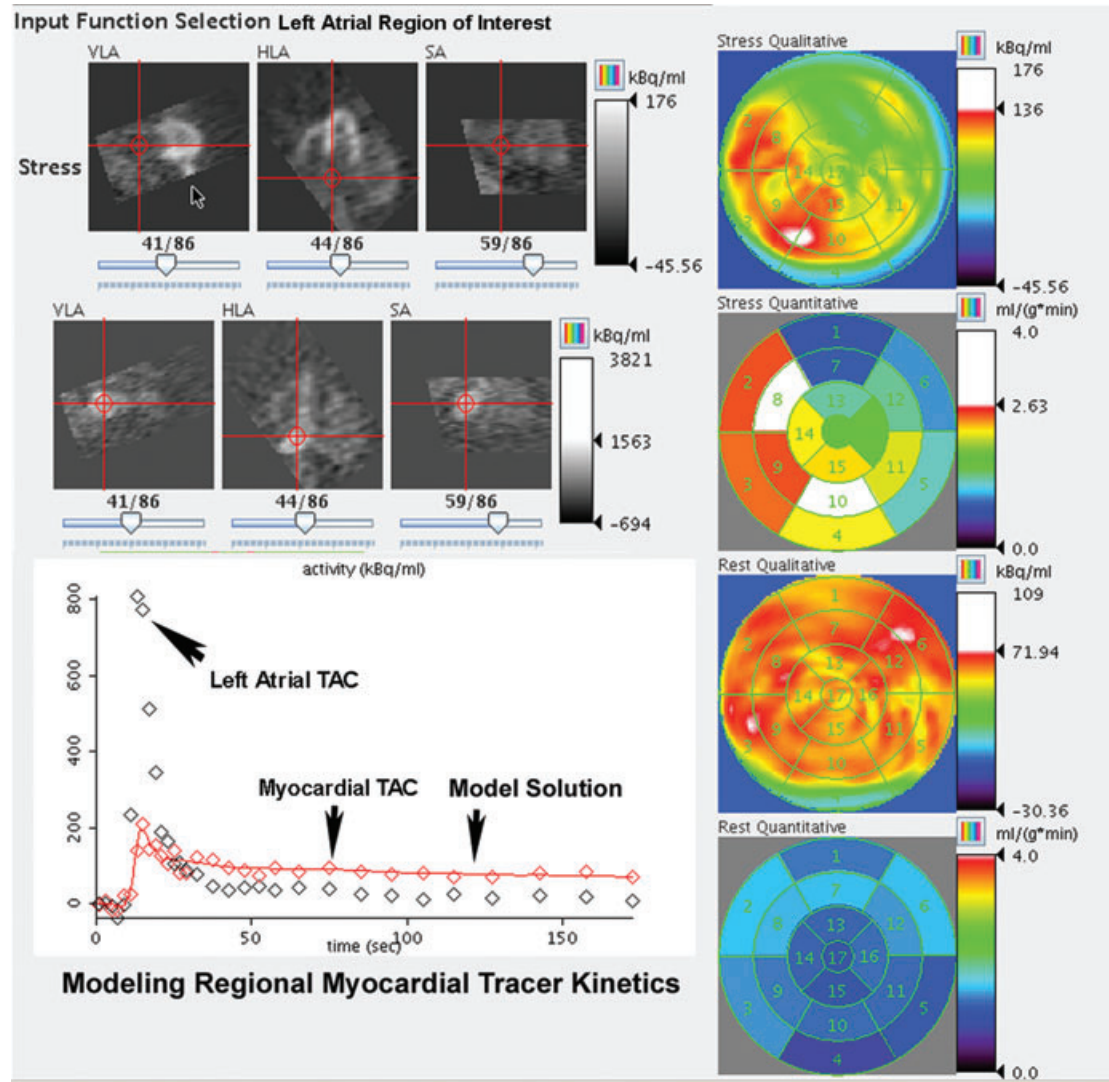


Figure 3. Composite of the interface to the Quantitative Perfusion Program showing positioning of cavity ROIs (*upper left figures*), the time–activity curves in the LA (serving as the input to the model), and the model fit to the TAC curve in an ROI (*bottom left figure*). The cumulative images from 40 to 180 s are shown as *bull’s-eye plots* with the cardiac apex at the center and the six basal ROIs at the circumference (*right*). During adenosine-induced stress the qualitative cumulative image (*top right*) shows a low-flow region in segments 1 and 2, and quantitative analysis (*second from top, right*) via the modeling provides the estimated flow there as $0.7 \text{ mL g}^{-1} \text{ min}^{-1}$. This is just half of the flow in these same ROIs during the resting state, $1.4 \text{ mL g}^{-1} \text{ min}^{-1}$ (*lower right two bull’s-eyes*). The *second and fourth bull’s-eyes* give quantitatively the average flows per gram of tissue within the 17 ROIs.

the left atrial or left ventricular cavity from which an input function time–activity curve (TAC) is generated. In the next step, the program automatically segments out the LV myocardium and generates 17 or 20 myocardial regions (based on American College of Cardiology criteria) for which TACs are gen-

erated (Fig. 3, left lower graph). A specific variant of the GENTEX model, implemented in JSim, then uses the cavity and myocardial TAC curves to estimate regional myocardial blood flow (rMBF) in all of the ROIs and generate polar plots of rMBFs at rest and during pharmacologic stress and of flow reserve

(stress rMBF/rest rMBF), as shown on the right side of Figure 3.

Modeling standards and model databases

Modeling standards are a subject of much interest in the modeling community. While JSim, CellML, SBML, and QKDB all have requirements and help to raise the standards of modeling, nevertheless it is not yet expected that models meet a gold standard. The particular virtue of JSim is that prior to compilation of the model code, the precompiler checks every equation for the balance of units and demands correctness before proceeding with compilation; this detects a multiplicity of errors that cannot be checked in standard procedural languages, such as C and MATLAB. The standards desired for our Physiome site, www.physiome.org, are provided there for review and improvement and at the IMAG website for the NIH/NSF Working Group 10 of the Multiscale Modeling Consortium at www.imagwiki.org/mediawiki/index.php?title=Main_Page. These proposed standards, or ones simplified to contain the most critical factors, will at some point be required for inclusion in databases, as is the intent for both the BioModels database and the University of Washington Physiome database.

The suggested standards include testing for adherence to conservation laws, the balances of mass, charge, chemical moieties, energy, volume, etc. These can be written into model programs on first principles. A most valuable asset in doing this is to have *units on every variable and parameter*. JSim provides both unit balance checking and automated unit conversion. Unit conversion means that one can use time in femtoseconds, seconds, minutes, or days, and these will all be converted to the basic unit (seconds in this case) without the programmer writing the conversion. The automatic unit balance checking on every equation reveals errors by alerts during compilation. The GENTEX model and the simpler models to which it can be reduced all pass the unit balance checking.

Conclusions

Multiscale modeling is an integrating tool for the analysis of organ function. The range of coverage is from cellular molecular reactions and the trapping of reaction products and the physics and mechanics of contraction to blood flow and the delivery

of tracer agents, substrates and oxygen to the organ and their heterogeneous spread throughout the organ. With modern computational speeds, realistic representation of the physiologic events can be achieved and thereby provide the physician with improved, quantitative information for diagnosis and therapy.

Acknowledgments

The research has been supported by NIH Grants HL19139 (heterogeneity studies), RR1243, and BE1973 (JSim), NSF Grant 0506477 (multiscale modeling), NIH Grants HL73598 and HL88516 (tutorial design).

Conflicts of interest

The authors declare no conflicts of interest.

References

1. Bassingthwaighte, J.B. & C.A. Goresky. 1984. Modeling in the analysis of solute and water exchange in the microvasculature. In *Handbook of Physiology. Sect. 2, The Cardiovascular System. Vol IV, The Microcirculation*. E.M. Renkin & C.C. Michel, Eds.: 549–626. American Physiological Society. Bethesda, MD.
2. Bassingthwaighte, J.B., C.Y. Wang & I.S. Chan. 1989. Blood-tissue exchange via transport and transformation by endothelial cells. *Circ. Res.* **65**: 997–1020.
3. Bassingthwaighte, J.B., I.S. Chan & C.Y. Wang. 1992. Computationally efficient algorithms for capillary convection-permeation-diffusion models for blood-tissue exchange. *Ann. Biomed. Eng.* **20**: 687–725.
4. Bassingthwaighte, J.B., C.A. Goresky & J.H. Linehan, Eds. 1998. *Whole Organ Approaches to Cellular Metabolism. Capillary Permeation, Cellular Uptake and Product Formation*. Springer Verlag, New York.
5. Bassingthwaighte, J.B., H. Qian & Z. Li. 1999. The Cardiome Project: an integrated view of cardiac metabolism and regional mechanical function. *Adv. Exp. Med. Biol.* **471**: 541–553.
6. Bassingthwaighte, J.B., G.R. Raymond, J.D. Ploger, *et al.* 2006. GENTEX, a general multiscale model for *in vivo* tissue exchanges and intraorgan metabolism. *Phil. Trans. Roy. Soc. A: Math. Phys. Eng. Sci.* **364**: 1423–1442.
7. Bassingthwaighte, J.B. 2006. A practical extension of hydrodynamic theory of porous transport for hydrophilic solutes. *Microcirculation* **13**: 111–118.

8. Caldwell, J.H., G.V. Martin, G.M. Raymond & J.B. Bassingthwaighe. 1994. Regional myocardial flow and capillary permeability-surface area products are nearly proportional. *Am. J. Physiol. Heart Circ. Physiol.* **267**: H654–H666.
9. Goresky, C.A. 1963. A linear method for determining liver sinusoidal and extravascular volumes. *Am. J. Physiol.* **204**: 626–640.
10. King, R.B., J.B. Bassingthwaighe, J.R.S. Hales & L.B. Rowell. 1985. Stability of heterogeneity of myocardial blood flow in normal awake baboons. *Circ. Res.* **57**: 285–295.
11. King, R.B., G.M. Raymond & J.B. Bassingthwaighe. 1996. Modeling blood flow heterogeneity. *Ann. Biomed. Eng.* **24**: 352–372.
12. Kuikka, J., M. Levin & J.B. Bassingthwaighe. 1986. Multiple tracer dilution estimates of D- and 2-deoxy-D-glucose uptake by the heart. *Am. J. Physiol. Heart Circ. Physiol.* **250**: H29–H42.
13. Li, Z., T. Yipintsoi & J.B. Bassingthwaighe. 1997. Non-linear model for capillary-tissue oxygen transport and metabolism. *Ann. Biomed. Eng.* **25**: 604–619.
14. Vink, H. & B.R. Duling. 1996. Identification of distinct luminal domains for macromolecules, erythrocytes, and leukocytes within mammalian capillaries. *Circ. Res.* **79**: 581–589.
15. Vinnakota, K. & J.B. Bassingthwaighe. 2004. Myocardial density and composition: A basis for calculating intracellular metabolite concentrations. *Am. J. Physiol. Heart Circ. Physiol.* **286**: H1742–H1749.
16. Wilke, N., K. Kroll, H. Merkle, *et al.* 1995. Regional myocardial blood volume and flow: First-pass MR imaging with polylysine-Gd-DTPA. *J. Magn. Res. Imaging* **5**: 227–237.